

The Effect of Rain and Flooding Events on AMSR-E Signatures of La Plata Basin, Argentina

Paolo Ferrazzoli, *Senior Member, IEEE*, Rachid Rahmoune, Fernando Moccia, Francisco Grings, Mercedes Salvia, Matias Barber, Vanesa Douna, Haydee Karszenbaum, Alvaro Soldano, Dora Goniadzki, Gabriela Parmuchi, Celina Montenegro, Patricia Kandus, and Marta Borro

Abstract—The objective of this paper is to describe and explain the effects on selected AMSR-E channels of two strong events, i.e., a rainstorm and a flooding, occurred in the Argentine section of La Plata basin. More specifically, the rainstorm took place within the Chaco region, which is covered by a continuous, moderately dense forest. The flooding affected the terminal part of Paraná River. The study is based on monitoring the temporal trends of the polarization indexes at various AMSR-E bands. In the forest, the rainstorm produces an effect on C band channels which is moderate, but well evident. The presence of this effect agrees with model simulations presented in previous papers. In the Paraná River, measurements of water level are available. Variations of polarization index at various frequencies are observed in correspondence with variations of water level in four different stations. However, the amount of the effect and the correlation between variables are dependent on the properties of the areas surrounding the stations. The Delta of Paraná river, where a land cover map is available, was selected for estimation of fraction of flooded area by using an algorithm available in the literature.

Index Terms—Flooding, forests, passive microwaves, soil moisture.

I. INTRODUCTION

THE use of passive microwave remote sensing to monitor soil and vegetation properties has been the subject of several studies in the recent decades. It is well known that soil moisture is a fundamental variable for environmental applications. A reliable monitoring of this variable is important for hydrologic and climatic models, and specially to assess the occurrence and the amount of drought and flood events. On the other hand,

Manuscript received February 27, 2009; revised November 26, 2009. Current version published February 24, 2010. This work was supported by the Consejo Nacional de Investigaciones Científicas y Técnicas (CONICET) PID 6109, and FonCyT/MINCYT PICT 14339 and 1203.

P. Ferrazzoli, R. Rahmoune, and F. Moccia are with the Tor Vergata University, Ingegneria-DISP, I 00133 Rome, Italy.

F. Grings, M. Salvia, M. Barber, V. Douna, and H. Karszenbaum are with the Instituto de Astronomía y Física del Espacio (IAFE), Ciudad Universitaria, Pabellón IAFE, Buenos Aires, Argentina.

A. Soldano and D. Goniadzki are with the Sistema de Alerta Hidrológico de la Cuenca del Plata, Instituto Nacional del Agua, Autopista Ezeiza Cañuelas, 1804, Ezeiza, Pcia. de Buenos Aires, Argentina.

G. Parmuchi and C. Montenegro are with the Secretaría de Ambiente y Desarrollo Sustentable, UMSEF, San Martín 451, C1004AAI, Buenos Aires, Argentina.

P. Kandus and M. Borro are with the Laboratorio de Ecología Teledetección y Ecoinformática, Instituto de Investigaciones e Ingeniería Ambiental (3iA.) Universidad Nacional General San Martín, San Martín, Prov. Buenos Aires, Argentina.

Color versions of one or more of the figures in this paper are available online at <http://ieeexplore.ieee.org>.

Digital Object Identifier 10.1109/JSTARS.2010.2040584

mapping and monitoring vegetation variables, such as biomass and Leaf Area Index (LAI), is important in the study of fundamental problems, such as global carbon cycle and climatic changes. From a physical point of view, the sensitivity of passive microwave measurements to soil and vegetation properties was proved by several theoretical and experimental investigations [1].

For bare soil, the emissivity at vertical (V) polarization is higher than the one at horizontal (H) polarization. Basically, an increase of soil moisture produces a decrease of emissivity at both polarizations, and at all microwave frequencies. However, the effect is more important at H polarization and at the lower frequencies [1]–[3]. On the other hand, a decrease of roughness produces effects which are similar to the ones produced by an increase of moisture. If the soil becomes smoother, a decrease of emissivity, which is more evident at H polarization and at lower frequencies, is observed [2]. In the presence of flooding events and/or strong rainstorms, the two effects can concur to reduce the emissivity, since the soil becomes wet and smoother at the same time. On its turn, the influence of vegetation is dependent on frequency, on the overall biomass and the geometrical properties of vegetation elements [4]. On average, vegetation growth produces a decrease of the difference between vertically polarized and horizontally polarized emission,

Several studies were aimed at singling out vegetation effects from soil effects. It was found that the polarization difference at high frequencies (Ka band) was mostly related to vegetation emission, and showed a good correlation with vegetation indexes derived by optical instruments [5]. Further studies adopted lower frequencies, typically X band. Moreover, in order to eliminate the dependence on surface temperature, a normalized polarization index [6] was defined. Experimental studies, confirmed by a simple zero order radiative transfer model, demonstrated that this index is sensitive to vegetation biomass [2], [6]. A further parametric study, carried out by means of a discrete physical model, confirmed the main finding of experimental studies and pointed out that the same polarization index is also sensitive to soil moisture, at least at frequencies lower than 10 GHz [7]. This dependence on soil moisture was confirmed by an experimental analysis of C band signatures collected at global scale by the SMMR radiometer [8].

The problem of discriminating between soil and vegetation effects can be mitigated by considerations about the specific application, as well as the spatial and temporal scales. When the objective of the satellite observation is to produce maps, spatial variations of polarization or frequency patterns are mostly

related to variations of vegetation properties. Similar considerations can apply for the case of long term, seasonal variations in time. However, short term variations of polarization and/or frequency properties of the emission, occurring after a rainstorm or a flooding, can be related to changes of soil properties. This is particularly true for the case of forests, in which the biomass changes very slowly. In the case of strong flooding, the polarization and frequency patterns may be affected also by a reduction of the emerged biomass.

Passive signatures collected by SMMR and SSM/I instruments were exploited for land applications. In these sensors, 37-GHz and 19-GHz channels were used, since lower frequencies were available only at very poor resolutions, or not available at all. Although high frequencies suffer atmospheric effects and high canopy attenuation, valid results in some applications were obtained. In [9], ten categories of vegetation cover were identified, and were associated to different histograms of polarized emissivity measured by SSM/I. A global study about flood dynamics was carried out by a synergic use of SSM/I signatures and data collected by AVHRR and ERS scatterometer [10]. In [11], the absolute polarization difference at 37 GHz proved to be correlated to vegetation density and was sensitive to flooding effects occurred in the Amazon River. This last application was further exploited in [12]–[14]. A simple algorithm, based on the polarization difference at 37 GHz measured by SMMR, was adopted to estimate the fraction of flooded area during several events occurred in the Amazon river and in other large South American rivers floodplains.

In the more recent years, the availability AMSR-E signatures offered new opportunities [15]. This sensor spans a wide range of frequencies, from 6.925 GHz to 89.0 GHz, and the spatial resolution is substantially improved with respect to previous ones. Based on AMSR-E data, useful algorithms have been developed to retrieve soil moisture [16], [17] and vegetation variables [18].

In this paper, AMSR-E signatures of two main ecosystems, a large dry forest (Chaco forest) and a wetland area of the Paraná River sub-basin were analyzed during the 2006–2007 time frame. The objective is to describe and explain the effects on selected AMSR-E channels of two strong events, a rainstorm and a flooding, occurred in the Argentine section of La Plata basin.

The rainstorm was observed in October 2006, after a long dry period, in a large area partially covered by the Chaco forest. The problem of monitoring soil moisture effects under forests is receiving great attention, also in view of the just recently launched ESA SMOS system with an L band radiometer, which is expected to have a better sensitivity to soil moisture variations. Some ground based experiments indicate that the effects of rain on the emission of dense forests are very low, even at L band [19], [20]. However, the soil was rather moist in these experiments, also before the rain event, which reduced the dynamic range. In other ground-based experiments, carried out over forests with moderate biomass, the effects of soil moisture variations on forest emission were detected [21]. In general, the available experimental data are not yet sufficient to draw reliable conclusions, and the availability of spaceborne results can contribute to the discussion about this topic. In this paper, we

show and interpret the moderate increase of polarization index observed after the rainstorm.

A strong flooding affected a region in the last part of the Paraná River sub-basin, for a total time of about two months. Evident effects on the polarization indexes were observed at all frequencies. In the case of moderate flooding, these effects find explanation in an increase of soil moisture and a decrease of soil roughness. When the flooding is severe, it produces also a decrease of the emerged biomass, with further increase of polarization indexes. The multitemporal trends of polarization indexes have been compared against the trends of measured water level in four different regions along the Paraná River. Finally, the fraction of flooded area in the Paraná River Delta has been estimated by applying the algorithm described in [12] and [13].

The following sections describe the area and discuss the observed AMSR-E features, taking into account the climatic events addressed and the land cover characteristics.

II. LA PLATA BASIN

The La Plata Basin (LPB) (Spanish: *Cuenca del Plata*) is the name given to the 3,100,000 km² hydrographical area that covers parts of Argentina, Brazil, Bolivia, Paraguay, and Uruguay. The precipitations falling within this area are collected by several rivers to finally reach the De La Plata River. The main contribution is due to the Paraná River and the Uruguay River, its two most important tributaries.

The LPB contains several key ecosystems. (1) The great Pantanal wetland, shared by Brazil, Bolivia, and Paraguay behaves as a regulator of the entire LPB hydrological system by slowing the flow of the Paraguay River's waters to the Paraná River, thus avoiding a conjunction of the maximum volume and flow rates from both rivers; (2) the highlands of both Paraguay and Paraná basins are important ecological corridors linking the Cerrados to the Pantanal; (3) the Cerrado biome covers about 2,000,000 km² of Central Brazil, 25% of the country's territory; (4) the Chaco region, another key ecosystem, is dominated by dry woodlands and savannas, and an alluvial area formed by the sediments of the Bermejo and Pilcomayo Rivers. This region constitutes a key ecological corridor among mountains, cloud forests (Yungas rainforests), high elevation deserts (Puna), and the shallow plains of the Chaco; (5) the Pampas is the ecosystem with the most fertile soils of the LPB, largely converted to agricultural production; (6) another important biome is the Atlantic Rainforest in the northeast of the LPB, characterized by intense deforestation and agricultural use.

One of the main issues of this large basin is to be able to monitor and predict the impact of global change and land use change on regional weather, climate, hydrology and agriculture production. Fig. 1 shows the extent of the La Plata Basin, each one of the countries sharing this region and main rivers.

A. Chaco Forest

“Gran Chaco Americano” is a wide forest area, spanning the North-East of Argentina and parts of Bolivia and Paraguay. The total extent is more than 100 million hectares. Within the area, there is a wide variability of climatic conditions

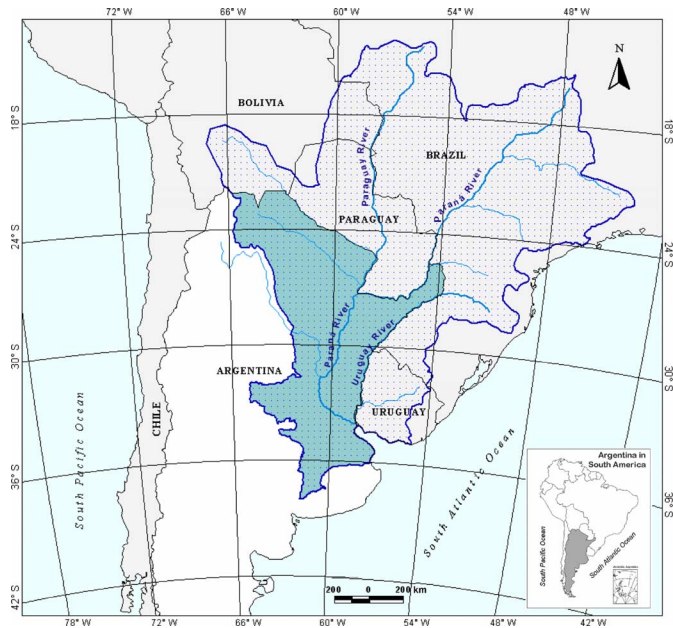


Fig. 1. La Plata basin location, extent, countries, and main rivers. Argentine sector is highlighted.

and botanical species. The event analyzed occurred in the semi-arid area (“Chaco semi-arido”) located approximately between 24°S and 27°S of latitude, 62°W and 64°W of longitude. This area is covered by a continuous, deciduous forest. There are several species, but the dominating ones are “Quebracho colorado santiagueño” (*Schinopsis quebracho colorado*) and “Quebracho Blanco” (*Aspidosperma quebracho blanco*). Although the forest is continuous, the biomass is moderate. Extensive measurements, with a sampling interval of 0.5° × 0.5°, indicate biomass values typically in the range 70–110 t/ha (7–10 kg/m²). There is a wide variability of tree dimensions. The average value of diameter at breast height is about 30 cm, but some trees show values higher than 100 cm.

In the lower part of this area (“Bajos Submeridionales”), a strong rainstorm occurred in October, 3, 2006. The amount of rainfall was between 50 and 150 mm. Since this event occurred after a long dry period of time, it is estimated that the variation of soil properties were very strong.

B. Parana Sub-Basin

The lower part of Parana River is subject to strong variations of water level, related to local rain events and the contribution of up-water of Paraná and Paraguay Rivers. Furthermore the terminal part of this sub-basin is influenced by the tidal regime of the La Plata estuary.

In particular, in the period from February to April, 2007, significant increases in the water level were observed in the sub-basin. Four monitoring stations have been considered. Their locations, as well as the centers of AMSR-E footprints, are shown in Fig. 2. Flooding events were observed in the regions along the river, which were particularly important in the areas close to the end, characterized by a flat topography and the dominance of herbaceous vegetation.

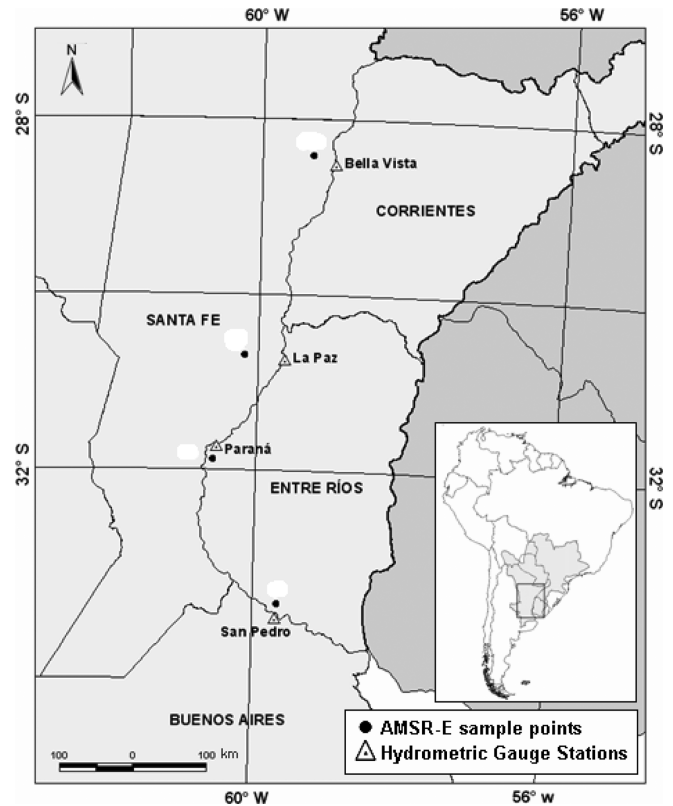


Fig. 2. Hydrological stations and centers of AMSR-E footprints (sample points) in the lower part of Paraná Basin.

In the area studied in this paper, the Paraná River main channel is surrounded by an extended floodplain. This floodplain is topographically lower than its surrounding areas, and is covered by a highly heterogeneous wetland with a complex landscape pattern. Nevertheless, at the spatial scale of AMSR-E it can be said that this wetland is dominated by lagoons, different communities of herbaceous vegetation in the extended lowlands, and the presence of forests (*Salix humboldtiana* and *Tessaria integrifolia*) in the levees (relative uplands) adjacent to the channels.

III. INSTRUMENT AND THE DATA SET

AMSR-E is a microwave radiometer operating at six frequency bands: 6.925 GHz (C), 10.65 GHz (X), 18.7 GHz (Ku), 23.8 GHz, 36.5 GHz (Ka), and 89.0 GHz [15], [22]. Lower frequencies are more suitable for terrestrial applications, while higher frequencies, i.e., 23.8 GHz, 36.5 GHz, and 89.0 GHz, are influenced by atmospheric water vapor and clouds. A conical scanning is used to observe the terrestrial surface with a local angle of 55°. The IFOV is equal to 43 × 75 km at 6.925 GHz, is reduced to 29 × 51 km at 10.65 GHz, and to 8 × 14 km at Ka band. The data are stored in Hierarchical Data Format (HDF), which is compatible with NASA HDF-EOS standard. In this study, we have used L1b data, which contain values of brightness temperature, at vertical (V) and horizontal (H) polarization, corrected and calibrated. Each file, is 80 Mb, contains brightness temperature values along a 1450 km strip. The data have been downloaded from NASA site <http://nsidc.org/ims-bin/pub/nph-ims.cgi/u885372>. We have

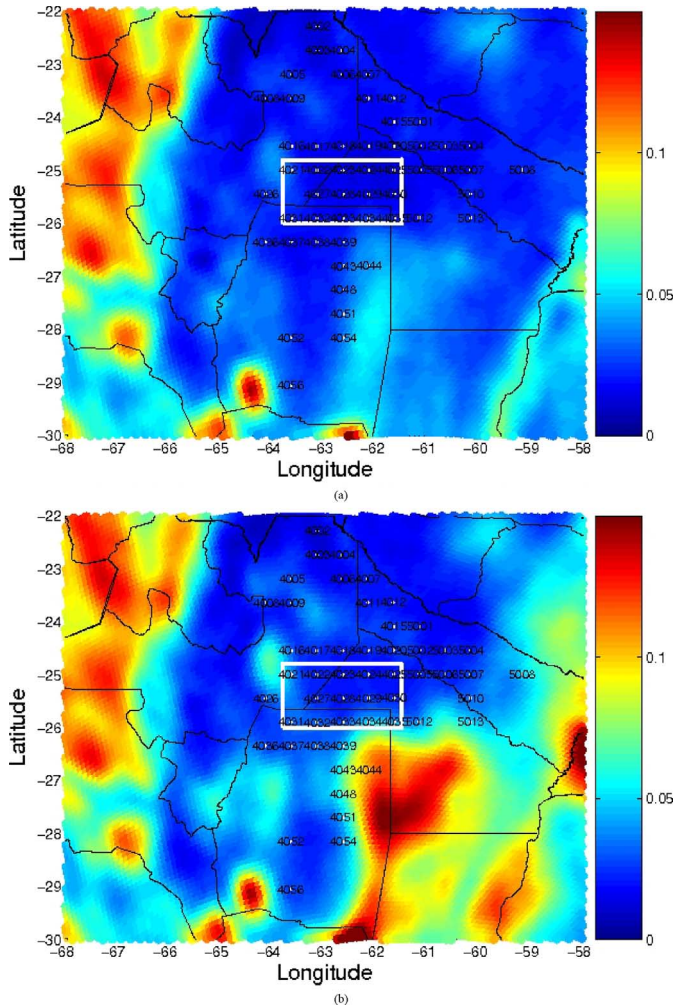


Fig. 3. General maps of PI at C band in the Chaco area. (a) September 18 (before rain). (b) October 4 (after rain). The continuous forest is indicated by the white box.

adopted a repetition time of 16 days, which corresponds to the exact repeat orbit, in order to evaluate variations occurred over footprints with the same location.

In the analysis, we have used the Polarization Index PI [11], which is defined as

$$PI = \frac{T_{bv} - T_{bh}}{0.5(T_{bv} + T_{bh})}. \quad (1)$$

T_{bv} and T_{bh} are the brightness temperature values collected at vertical and horizontal polarization, respectively. This index has been evaluated at C, X, and Ka bands.

IV. MONITORING THE RAINSTORM IN CHACO FOREST

For the Chaco forest, the effects of the heavy rainstorm on the polarization index have been evaluated. Ka band was not suitable in this study due to the influence of clouds.

General maps of PI at C band are shown in Fig. 3. The maps are based on AMSR-E observations of September 18 (before the rainstorm) and October 4 (soon after the rainstorm). The box indicates a region covered by a continuous forest, and the dots refer to sites where measurements of tree density, dry biomass and distribution of trunk diameters are available.

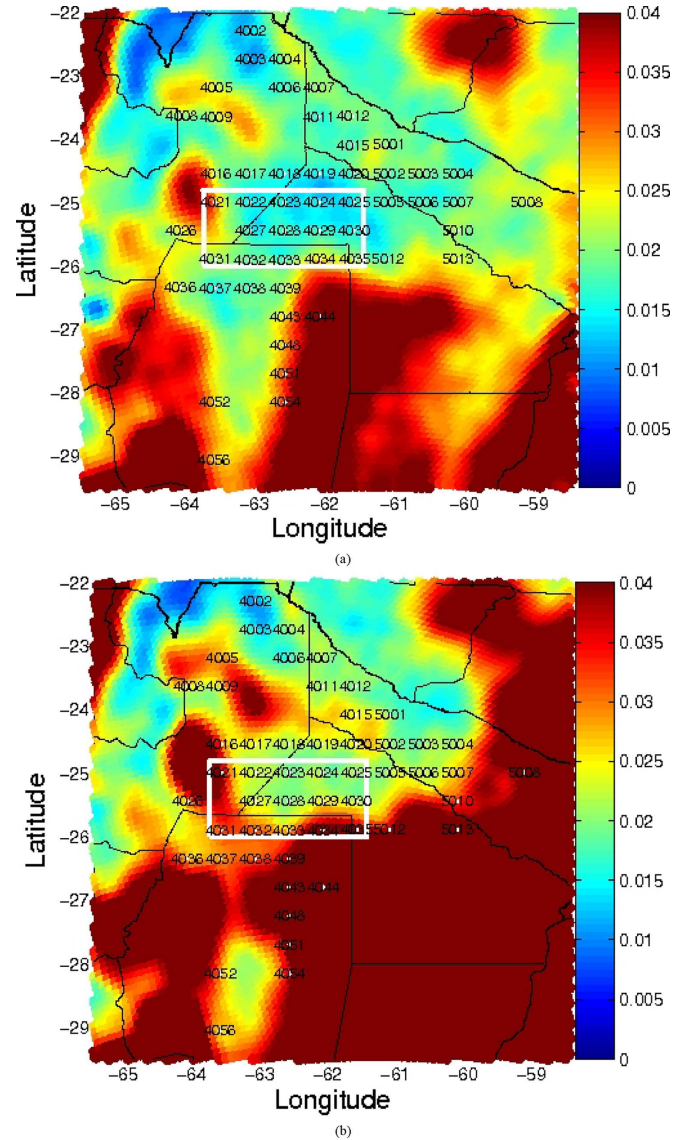


Fig. 4. Specific maps of PI at C band in the Chaco forest. (a) September 18 (before rain). (b) October 4 (after rain). The continuous forest is indicated by the white box. White dots indicate sites of measurements.

Measurements were provided by the Forest Evaluation System Management Unit (UMSEF) (<http://www.ambiente.gov.ar/?id-seccion=44>). The distance between points corresponds to about 0.5° in longitude and latitude. This PI map is extended to a large region, and the color scale is selected in order to detect PI values as high as 0.15. It is evident that, in the South East part of the area, mostly covered by herbaceous low vegetation, the PI showed extremely high increases after the rainstorm. However, it is difficult to appreciate variations within the forest, with this scale.

In Fig. 4, the comparison between the C Band PI's of the same dates is shown by using a more detailed map and a scale which saturates when the PI is equal to 0.04. With this representation, appreciable variations are observed even within the continuous forest, especially in the southern part. Before the rain event (September 18), the PI is quite uniform within the rectangular box. Although the ground measurements indicate that the biomass varies in a range between about 70 and 110 t/ha,

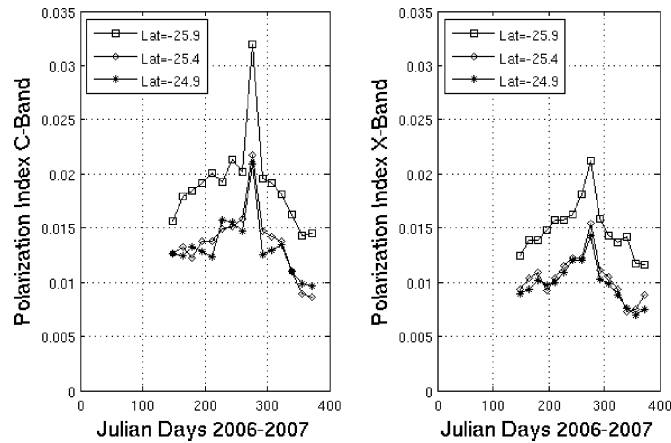


Fig. 5. Trends of Polarization Index within the Chaco forest at three latitudes. Left: C band. Right: X band.

the effects of this variation cannot be appreciated. It must be considered that measurements were carried out in specific locations, while the coarse resolution of the instrument creates a smoothing effect. After the rain event, a general increase of PI is observed in the whole area, associated to a gradient from the southern to the central part of the forest.

In Fig. 5, the trends of PI versus time are represented for a period of about 200 days. The PI was estimated by averaging over forest pixels belonging to the same latitude. Three latitudes, i.e., -25.9° , -25.4° and -24.9° , have been considered. The first latitude is just at the edge of the forest, while the other two correspond to internal parts. A peak on Day of Year 277 (i.e., October 4) is well evident for the samples of the lower latitude and, to a lesser extent, for the other samples. After the rain event, the PI values decrease again to values close to the ones they had before the event. For sake of comparison, the trends of PI at both C band and X band, are shown, for the same pixels. The trends of X band are similar to the ones of C band, but with a lower dynamic range due to the higher canopy attenuation. Anyhow, this comparison confirms the assumption that the effect is related to a change of soil properties after the rainstorm, and is not due to eventual artifacts of C band channel.

It can be concluded that the severe rainstorm produced variations of polarization index which are not negligible, although moderate. This result can be justified by some considerations. First of all, the forest was continuous, but not very dense. Ground measurements indicated that the biomass ranged between about 70 and 110 t/ha. Moreover, the rain event occurred after a long dry period. Therefore, it produced a strong variation of soil conditions. Finally, the event occurred at the end of winter, when the deciduous forest was not yet leafy. This last consideration is important. In fact, the canopy attenuation was mostly due to branches. Previous model studies indicated that branch attenuation is dominant at lower frequencies (e.g., L band), but increases as a function of frequency much more gently than leaf attenuation [23]. Various experimental results confirmed this property [21], [24], [25].

Other studies confirm that, for forests with moderate biomass, the contribution of soil emission is still appreciable at L and C bands [26].

V. MONITORING THE FLOODING IN THE LOWER PARANÁ

During the period of observations, important flood events took place in the Paraná sub-basin. The potential of previously defined PI indexes to monitor flooding events has been investigated. As expected, flooding produces an increase of PI, related to a strong increase of soil moisture and, in the extreme cases, to a reduction of emerged vegetation.

Fig. 6 shows maps of PI over a large region including the lower Paraná. Four AMSR-E channels have been considered. The maps shown on the left were obtained by using Ka band at high resolution (8×14 km). The other three maps were obtained at low resolution (43×75 km), and at Ka, X and C bands. For all channels, the maps on top, middle and bottom show PI on February 8 (low water level), PI on April 13 (high water level), and the difference, respectively. In agreement with previous observations [12]–[14] water bodies show a PI higher than 0.2, which corresponds to an absolute difference between V and H polarization equal to about 60 K. At Ka band, higher PI values are observed along the river (on February 8) and in the Delta (on April 13), but much lower values are observed in the surrounding areas. As expected, the contours of permanently or temporarily flooded areas are better delineated in the high resolution image. However, large scale variations are observed also at the low AMSR-E resolution. At the lower frequencies, the transition between higher and lower PI values is more gradual. There are wide areas in which the PI, was low on February 8, and increased to values higher than 0.1 on April 13. These are large agricultural areas, in which an increase of soil moisture can be more easily detected at lower frequencies, particularly at C band.

In order to evaluate more specifically the variations of the PI as a function of time, the four specific locations of Fig. 2 have been evaluated. For each point, the closest AMSR-E pixel has been considered. In Fig. 7, the temporal trends of water level are compared with the ones of PI at C and Ka bands.

To compare the effects of Paraná River water level on the PI for each selected station, we cannot consider only the absolute value of water level. Since the river channel has different characteristics in each zone (different width, maximum depth and bathymetry), we have to use some kind of measure to understand what the water level means in terms of floodplain soil condition. Since there is no accurate model of the topography of the floodplain all along the river, the only available data in all the stations is the alert level given by the National Water Institute for the nearby cities. It is important to remark that these values are computed for the evaluation of the effect of river water levels over the cities, and since, floodplains are topographically lower than the surrounding cities, when the river reaches the alert level, the floodplains have already been affected. It is a fair approximation to say that the water level in which the river starts inundating the floodplain is between 50 cm and 1 m lower than the alert level for the cities. With these assumptions, we analyzed each one of the graphs of Fig. 7. Table I shows, for each of the four stations, the maximum water level, the floodplain alert level and the corresponding days of inundation. These data are also indicated in Fig. 7 by means of horizontal and vertical lines. In all stations,

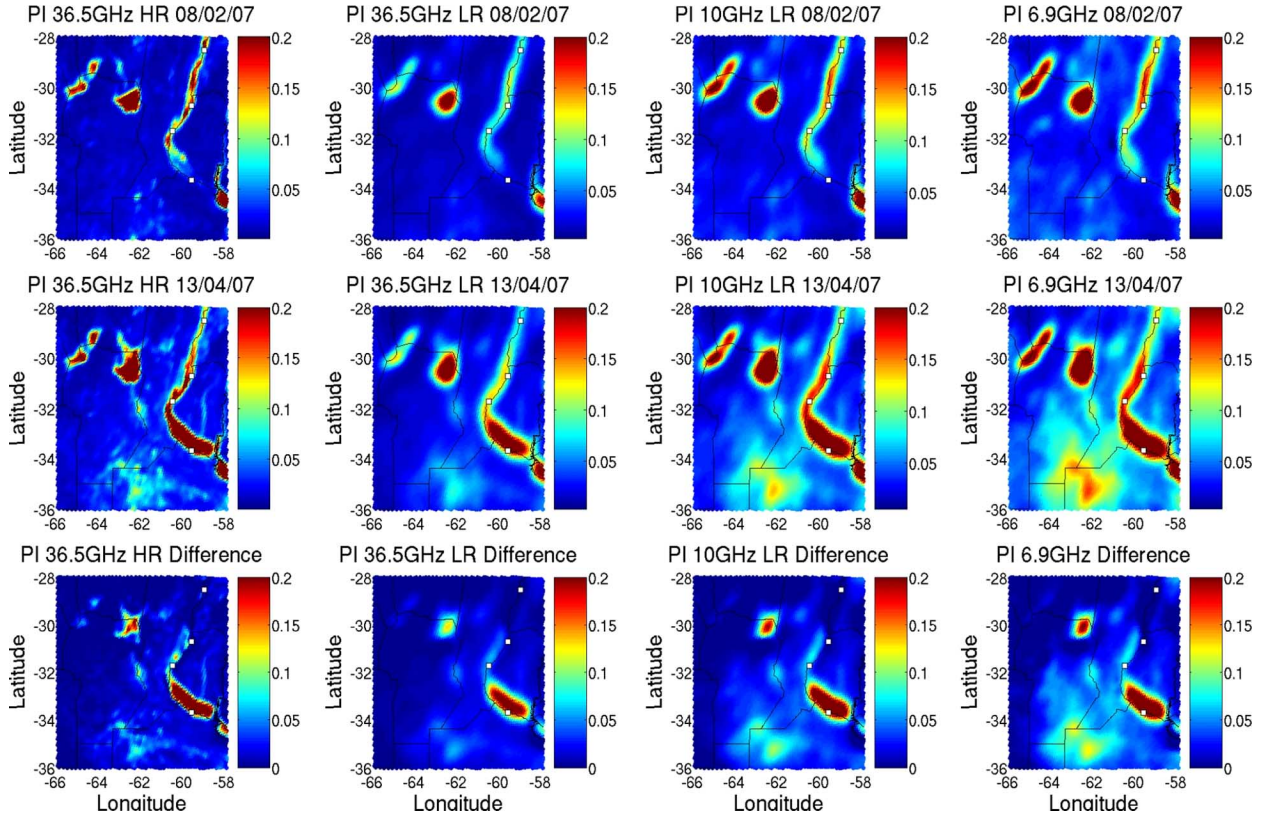


Fig. 6. Maps of PI in the lower part of Paraná River. From top to bottom: February 8, 2007 (before flooding), April 13, 2007 (after flooding), difference. From left to right: Ka band high resolution, Ka band low resolution, X band, C band. White squares indicate the locations of water level stations.

the inundation is associated to an increase of PI at both frequencies. The effect is more evident in San Pedro because the area is very flat and several precipitation events took place during the inundation period. After inundation, the PI at Ka band decreases rapidly, while the PI at C band decreases more slowly. Moreover, Ka band trends show some decreases of PI which are not associated to variation of soil properties, but to the presence of heavy clouds and rain. Although less pronounced, a similar behavior is observed in Bellavista, La Paz and Paraná. The inundation period indicated in Table I agrees very well with PI trends.

For the Paraná River Delta area, where a detailed map of land covers is available, we have estimated the fraction of flooded area using the algorithm described in [12] and [13]. The selected area, which is close to San Pedro station, is indicated in Fig. 8. The algorithm estimates the fraction of flooded area as a function of the absolute difference between vertically and horizontally polarized brightness temperatures (ΔT) measured at 36.5 GHz and at high resolution. The fractional inundation area is estimated using linear mixing models that account for the microwave emission of the major land covers within the subregion [12]. The model has three end-members that represent the contributions of water, nonflooded land, and inundated floodplain to the total ΔT

$$\Delta T_{\text{obs}} = f_w \Delta T_w + f_{n_f} \Delta T_{n_f} + f_f \Delta T_f \quad (2)$$

$$1 = f_w + f_{n_f} + f_f \quad (3)$$

where ΔT_{obs} is the ΔT observed by the radiometer, f_w , f_{n_f} and f_f are the fractional areas of open water (rivers and lakes without emergent vegetation), nonflooded land, and seasonally flooded land, respectively, and ΔT_w , ΔT_{n_f} , and ΔT_f are the ΔT values for open water, nonflooded land, and seasonally flooded land. Simultaneous solution of (2) and (3) yields the following equation for the fraction of inundated floodplain (f_f):

$$f_f = \frac{\Delta T_{\text{obs}} - f_w \Delta T_w - \Delta T_{n_f}}{\Delta T_f - \Delta T_{n_f}} \quad (4)$$

The fractional area of flooded land expands during inundation with a concomitant reduction in the fractional area of nonflooded land. The algorithm is based on the following considerations.

1. The temperature difference of water bodies, ΔT_w , is known. This value was set equal to 60 K. This is in agreement with [12], [13] and our measurements.
2. The temperature difference of nonflooded land, ΔT_{n_f} , must be a constant value for all the nonflooded vegetation types present in the area and can be estimated from images. In our case, this value was obtained using a high resolution landcover map of the Paraná River Delta derived from images acquired by the SAC-C MMRS satellite system [27]. First, the non flooded areas were determined, and then using this information in conjunction with AMSR-E images, ΔT_{n_f} was empirically determined as 4.2 K. This is in agreement with [12], [13].

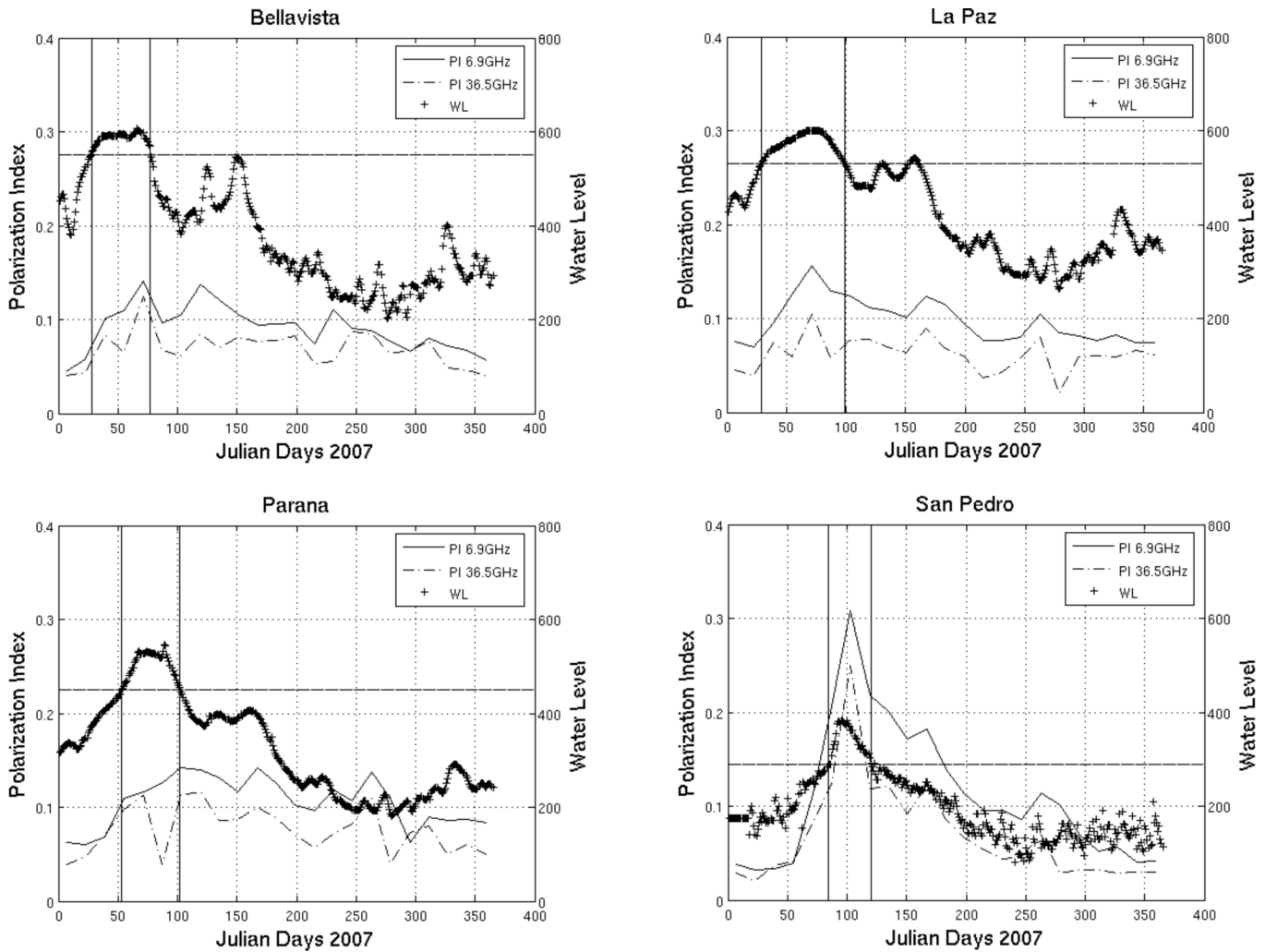


Fig. 7. Temporal trends of measured water level, Polarization Index PI at C band, and Polarization Index at Ka band for four locations in the lower part of Paraná River. Horizontal lines indicate floodplain alert level. Vertical lines indicate the beginning and end of the inundation period.

TABLE I
MAIN INUNDATION DATA IN THE FOUR WATER LEVEL STATIONS

	Bellavista	La Paz	Parana	San Pedro
Maximum water level (cm)	603	601	546	382
Floodplain alert level (cm)	550	530	450	290
Days of inundation (in year 2007)	28 - 77	29 - 99	53 - 102	84 - 120

3. The fractional area of permanent water bodies must be a constant and is assumed to be known. This value was estimated for the selected area using the available landcover map and it was found to be of the order of ~ 0.05 .
4. The temperature difference of flooded land, ΔT_f , must be a constant value for all the flooded vegetation types present in the area and can be estimated from images. The estimation of this value is a critical part of the algorithm and presents large variations as reported in [12]. The estimation of this parameter is complex since it is very difficult to find an homogeneously covered vegetated pixel of this dimension ($\sim 100 \text{ km}^2$ for Ka band). For our area, this value was estimated using the hydrometric values of San

Pedro station and ancillary information. The hydrometric peak for this area was observed on April 10 (see Fig. 7). At this date, this area was completely flooded ($\sim 90 \text{ cm}$ above the alert level). Therefore, for this date, we assume $f_f = 1 - f_w = 0.95$. Using (4), this leads to $\Delta T_f \sim 51 \text{ K}$. The trend of the fraction of flooded area is shown in Fig. 9. There is a general correspondence between the variations of flooded area and variations of water level measured in San Pedro. In spite of the high frequency of the selected AMSR-E channel, the algorithm works well, because for the area considered, the dominant vegetation type is herbaceous (mostly wetlands, maximum vegetation height $\sim 2 \text{ m}$) and they were submerged during the

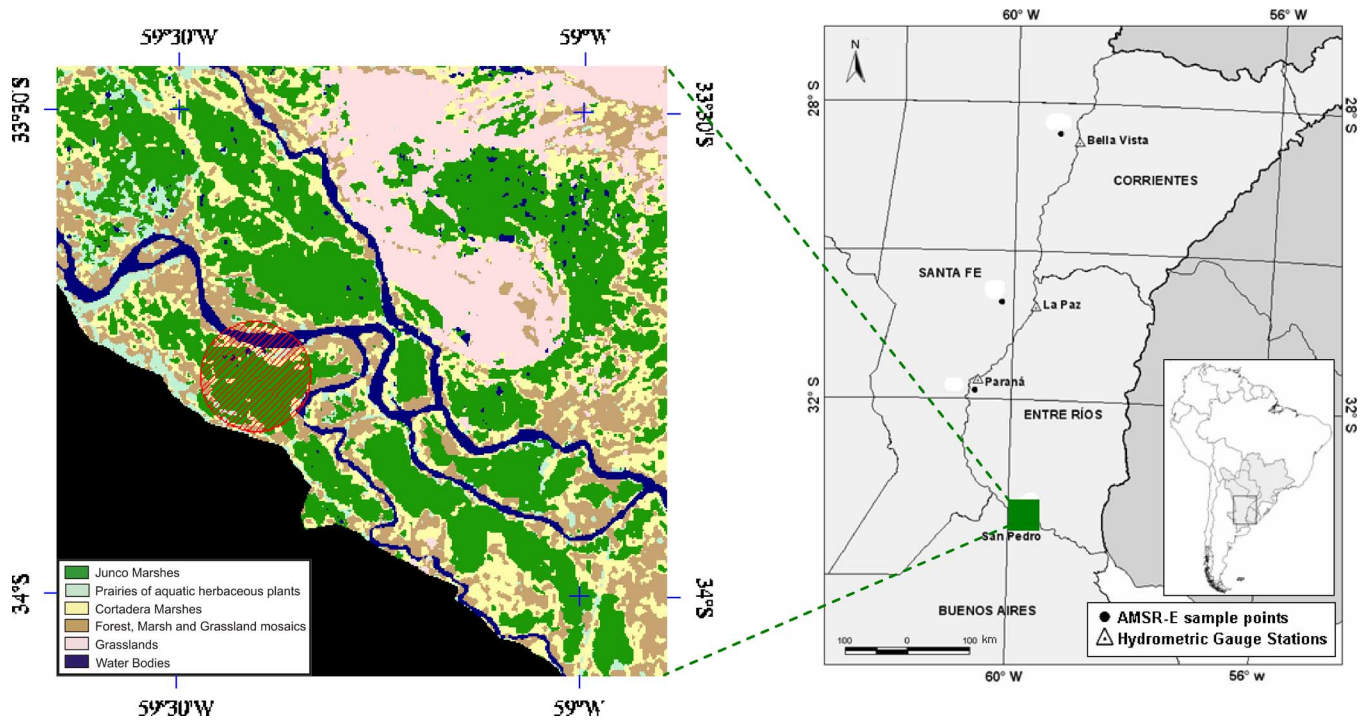


Fig. 8. Region where the algorithm to retrieve fraction of flooded area was applied. This region corresponds to the Paraná River Delta, near San Pedro city (right), an area where large floods are usual. This area was heavily affected by the April 2007 flood event. The area corresponding to the selected AMSR-E pixel is marked as a circle crossed by lines (left).

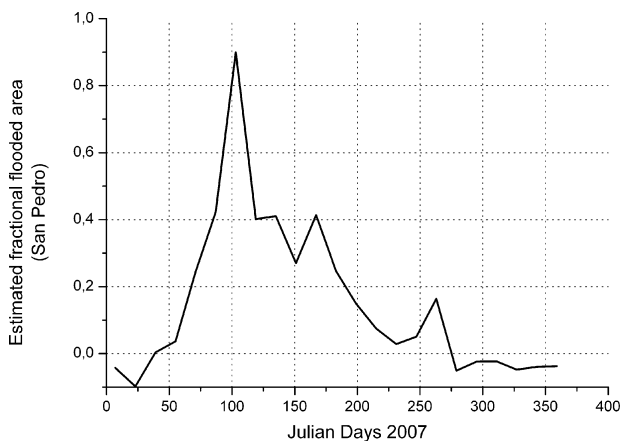


Fig. 9. Temporal trend of the fraction of flooded area in San Pedro region, estimated by using the algorithm of [12] and [13].

flooding. Some very low negative values of f_f are related to algorithm artifacts. This problem was also observed in [12], [13].

VI. CONCLUSION

The time trends of the polarization indexes, based on AMSR-E measurements at various channels from C to Ka band, have been analyzed during a rainstorm and a long lasting flooding. The rainstorm occurred in the Chaco forest, while the flooding was observed in the lower part of Paraná River basin.

Within the Chaco forest, the rainstorm produced an increase of the polarization index at C band, which was more evident in the Southern part of the forest area. This result can be explained by considering that the forest is moderately dense

(70 – 110 Tn/ha), although it is continuous, and the event occurred at the end of winter, when the deciduous trees were not leafy. Moreover, the initial soil moisture was low, due to a long dry period. This result can have some interest, since the problem of detecting soil moisture variations under forests is receiving attention and it is still under investigation.

Previous works indicated that passive microwave measurements are capable to monitor large basin for hydrological purposes. The flooding recorded by AMSR-E along the Paraná floodplain confirms that these measurements constitute a very useful tool for monitoring regional events. Increases of measured water level are associated to increases of polarization indexes. This area constitutes a complex and non uniform floodplain. The temporal pattern of the indexes is related to the floodplain characteristics, condition and climate behavior in each site. In the case of San Pedro, where heavy rains (over 400 mm) took place along March, the indexes evolve with a time pattern which is similar to the one of water level. The time pattern of fraction of flooded area, estimated by the algorithm of [12] and [13], shows a similar trend. This result is expected, since the flooded area has a known dependency to observed ΔT . Although theoretically simple, in the case of marshes, this algorithm at Ka band is able to capture the most relevant properties of the ΔT trends, and associate them to changes of water level. In summary this algorithm, feeded by on site estimation of key parameters, produces a reliable estimate of fraction of flooded area. This result has an important outcome, considering the importance of flood monitoring to mitigate environmental and social problems. In the future, it is expected that the system performance will improve, because the spatial resolution of spaceborne radiometers will be enhanced, also at lower frequencies, Moreover, also

systems operating at L band will be available (SMOS and future SAC-D/Aquarius and SMAP), with consequent reduction of vegetation attenuation. Therefore, more reliable results will be available for a larger set of land covers.

ACKNOWLEDGMENT

The authors would like to thank Dr. J. Borus from the National Water Institute (INA) for his useful comments and suggestions. They would also like to thank anonymous reviewers for their constructive comments resulting in an improvement of the paper.

REFERENCES

- [1] F. T. Ulaby, R. K. Moore, and A. K. Fung, *Microwave Remote Sensing, Active and Passive*. Dedham, MA: Artech House, 1986, vol. 3, From Theory to Applications.
- [2] S. Paloscia, P. Pampaloni, L. Chiarantini, P. Coppo, S. Gagliani, and G. Luzi, "Multifrequency passive microwave remote sensing of soil moisture and roughness," *Int. J. Remote Sens.*, vol. 14, pp. 467–483, 1993.
- [3] Y. K. Kerr and E. G. Njoku, "A semiempirical model for interpreting microwave emission from semiarid land surfaces as seen from space," *IEEE Trans. Geosci. Remote Sens.*, vol. 28, pp. 384–393, 1990.
- [4] T. J. Jackson and T. J. Schmugge, "Vegetation effects on the microwave emission from soils," *Remote Sens. Environ.*, vol. 36, pp. 203–212, 1991.
- [5] B. J. Choudhury and C. J. Tucker, "Monitoring global vegetation using Nimbus-7 37 GHz data: Some empirical relations," *Int. J. Remote Sens.*, vol. 8, pp. 1085–1090, 1987.
- [6] S. Paloscia and P. Pampaloni, "Microwave polarization index for monitoring vegetation growth," *IEEE Trans. Geosci. Remote Sens.*, vol. 26, pp. 617–621, 1988.
- [7] P. Ferrazzoli, L. Guerriero, S. Paloscia, P. Pampaloni, and D. Solimini, "Modelling polarization properties of emission from soil covered with vegetation," *IEEE Trans. Geosci. Remote Sens.*, vol. 30, pp. 157–165, 1992.
- [8] S. Paloscia, G. Macelloni, E. Santi, and T. Koike, "A multifrequency algorithm for the retrieval of soil moisture on a large scale using microwave data from SMMR and SSM/I satellites," *IEEE Trans. Geosci. Remote Sens.*, vol. 39, pp. 1655–1661, 2001.
- [9] C. Prigent, W. B. Rossow, and E. Matthews, "Global maps of microwave land surface emissivities: Potential for land surface characterization," *Radio Sci.*, vol. 33, pp. 745–751.
- [10] C. Prigent, F. Papa, F. Aires, W. B. Rossow, and E. Matthews, "Global inundation dynamics inferred from multiple satellite observations," *J. Geophys. Res.*, vol. 112, 1993–2000.
- [11] B. J. Choudhury, "Monitoring global land surface using nimbus-7 37 GHz data, Theory and examples," *Int. J. Remote Sens.*, vol. 10, pp. 1579–1605, 1989.
- [12] S. J. Sippel, S. K. Hamilton, J. M. Melack, and B. Choudhury, "Determination of inundation area in the Amazon River floodplain using the SMMR 37 GHz polarization difference," *Remote Sens. Environ.*, vol. 48, pp. 70–76, 1994.
- [13] S. J. Sippel, S. K. Hamilton, J. M. Melack, and E. M. M. Novo, "Passive microwave observations of inundation area and the area/stage relation in the Amazon River floodplain," *Int. J. Remote Sens.*, vol. 19, pp. 3055–3074, 1998.
- [14] S. K. Hamilton, S. J. Sippel, and J. M. Melack, "Comparison of inundation patterns among major South American floodplains," *J. Geophys. Res.*, vol. 107, no. D20, DOI:10.1029/2000JD000306, p. 8038, 2002.
- [15] T. Kawanishi, T. Sezai, Y. Ito, K. Imaoka, T. Takeshima, Y. Ishido, A. Shibata, M. Miura, H. Inahata, and R. Spencer, "The advanced microwave scanning radiometer for the earth observing system (AMSR-E) NASA's contribution to the EOS for global energy and water cycles studies," *IEEE Trans. Geosci. Remote Sens.*, vol. 41, pp. 184–194, 2003.
- [16] E. G. Njoku, T. Jackson, V. Lakshmi, T. Chan, and S. V. Nghiem, "Soil moisture retrieval from AMSR-E," *IEEE Trans. Geosci. Remote Sens.*, vol. 41, pp. 215–229, 2003.
- [17] S. Paloscia, G. Macelloni, and E. Santi, "Soil moisture estimates from AMSR-E brightness temperatures by using a dual-frequency algorithm," *IEEE Trans. Geosci. Remote Sens.*, vol. 44, pp. 3135–3144, 2006.
- [18] E. G. Njoku and T. K. Chan, "Vegetation and surface roughness effects on AMSR-E land observations," *Remote Sens. Environ.*, vol. 100, pp. 190–199, 2006.
- [19] M. Guglielmetti, M. Schwank, C. Mätzler, C. Oberdörster, J. Vanderborght, and H. Flüßler, "FOSMEX: Forest soil moisture experiments with microwave radiometry," *IEEE Trans. Geosci. Remote Sens.*, vol. 46, pp. 727–735, 2008.
- [20] J. P. Grant, J.-P. Wigneron, A. A. Van de Griend, A. Kruszcwsky, S. S. Søbjaerg, and N. Skou, "A field experiment on microwave forest radiometry: L-band signal behaviour for varying conditions of surface wetness," *Remote Sens. Environ.*, vol. 109, pp. 10–19, 2007.
- [21] E. Santi, S. Paloscia, P. Pampaloni, and S. Pettinato, "Ground-based microwave investigations of forest plots in Italy," *IEEE Trans. Geosci. Remote Sens.*, vol. 47, pp. 3016–3025, 2009.
- [22] C. L. Parkinson, "Aqua: an earth-observing satellite mission to examine water and other climate variables," *IEEE Trans. Geosci. Remote Sens.*, vol. 41, pp. 173–183, 2003.
- [23] P. Ferrazzoli and L. Guerriero, "Passive microwave remote sensing of forests: A model investigation," *IEEE Trans. Geosci. Remote Sens.*, vol. 34, pp. 433–443, 1996.
- [24] C. Mätzler, "Microwave transmissivity of a forest canopy: Experiments made with a beech," *Remote Sens. Environ.*, vol. 48, pp. 172–180, 1994.
- [25] M. Guglielmetti, M. Schwank, C. Mätzler, C. Oberdörster, J. Vanderborght, and H. Flüßler, "Measured microwave radiative transfer properties of a deciduous forest canopy," *Remote Sens. Environ.*, vol. 109, pp. 523–532, 2007.
- [26] A. D. Vecchia, P. Ferrazzoli, L. Guerriero, R. Rahmoune, S. Paloscia, S. Pettinato, and E. Santi, "Modeling the multifrequency emission of broadleaf forests and their "Components";," *IEEE Trans. Geosci. Remote Sens.*, vol. 42, pp. 260–272, 2010.
- [27] M. Salvia, H. Karszenbaum, P. Kandus, and F. Grings, "Datos satelitales ópticos y de radar para el mapeo de ambientes en macro-sistemas de humedal," *Revista de Teledeteccion*, vol. 31, pp. 35–51, 2009.



Paolo Ferrazzoli (M'94–SM'06) graduated from the University "La Sapienza" of Rome, Italy, in 1972.

In 1974, he joined Telespazio s.p.a., where he was mainly active in the fields of antennas, slant-path propagation, and advanced satellite telecommunication systems. In 1984, he joined Tor Vergata University of Rome, where he is presently working, teaching microwaves and propagation. His research here is focused on microwave remote sensing of vegetated terrains, with particular emphasis on electromagnetic modeling. He has been involved

in international experimental remote sensing campaigns such as AGRISAR, AGRISCATT, MAESTRO-1, MAC-Europe, and SIR-C/X-SAR. He has participated in the coordinating team of ERA-ORA Project, funded by EEC, establishing an assemblage among several European researchers working in radar applications. He has been a member of the Science Advisory Group of ESA SMOS Project.



Rachid Rahmoune received the degree in physics in 2000 from HASSAN II University of Casablanca, Morocco, the M.S. degree in space systems on earth observation, application to remote sensing, in 2002 from ISUFI, University of Lecce, Italy. He is currently pursuing the Ph.D. degree in geoinformation at Tor Vergata University, Rome, Italy, working on a thesis focused on the "validation and extension of emissivity and reflectivity models for forests at microwaves", with applications to the SMOS mission.

From 2003 to 2007, he was with the Remote sensing Group, Department of Physics, University and Polytechnic of Bari, Italy. His activity was focused on the monitoring of coastal areas and the use of SAR interferometry in the generation of DEM and permanent scatterers.



Fernando Moccia received the degree in telecommunications engineering in 2008, from Tor Vergata University, Rome, Italy.

In 2007, he worked in cooperation with IAFE (Instituto de Astronomía y Física del Espacio) in Buenos Aires, Argentina, on the monitoring of flooding events at large-scale with the use of passive radiometers.



Alvaro Soldano is a Specialist in remote sensing and geographical information resources systems applied to environmental research (UNLU), naval and mechanic engineering (UBA), SIAH researcher staff (1983/2009). He is on the Staff of the Executive and Technical Direction of the National Commission on Space Activities (CONAE) of Argentina (2009/2010). He has extensive experience in hydrology and satellite data applications in emergencies.



Francisco Grings received the Ph.D. degree in 2008.

He is a physicist and junior researcher, forward and inverse models, with Consejo Nacional de Investigaciones Científicas y Técnicas (CONICET), Instituto de Astronomía y Física del Espacio (IAFE), Buenos Aires, Argentina. He is responsible for remote sensing modeling within IAFE's group. He is leading the Observing System Simulation Experiment (OSSE) project at IAFE.



Dora Gonizadski is currently Director of the Centro de Sistemas de Información y Alerta Hidrológico (SIAH) of the National Water Institute (INA), responsible for producing hazard maps and prediction maps of hydrological variables. Her interests are operational hydrology, hydrological and hydraulic modeling for simulation and forecast, real-time monitoring of hydrometeorological parameters, emergency management, the development of warning systems, and project management for hydrological emergencies.



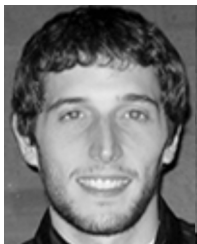
Mercedes Salvia is a biologist currently pursuing the Ph.D. degree in wetlands ecology at the Instituto de Astronomía y Física del Espacio (IAFE), Buenos Aires, Argentina.

She has been producing land cover land use maps with optical data and she is responsible of monitoring and mapping the effects of extreme events (floodings and burnings) in the Paraná wetlands using optical and radar data. She is also participating in passive microwave applications in La Plata Basin.



Gabriela Parmuchi is a biologist and remote sensing and GIS expert with UMSEF.

Since 2001, she has been on the staff of the Native Forest Division where she is working in mapping native forests.



Matias Barber is a physicist currently pursuing the Ph.D. degree in surface scattering at the Instituto de Astronomía y Física del Espacio (IAFE), Buenos Aires, Argentina.

He joined IAFE one year ago, where he is responsible for field work and surface modeling.

Celina Montenegro works in engineering in agronomy, responsible for producing rates of deforestation of native Chaco forest, at UMSEF. She is the technical coordinator of the Native Forest Division at the Secretaría de Medio Ambiente.

Vanesa Douna, photograph and biography not available at the time of publication.



Patricia Kandus works in ecology, field work, architectural vegetation models, remote sensing, and is a wetland expert at UNSAM. She was with the University of Buenos Aires, Argentina, in wetland ecology for over ten years and is presently with UNSAM, where she is directing the Ecology and Remote Sensing Group focused on remote sensing of wetland vegetation structure and dynamics.



Haydee Karszenbaum is a physicist and research member of Consejo Nacional de Investigaciones Científicas y Técnicas (CONICET), a remote sensing specialist, and Director of the remote sensing group at the Instituto de Astronomía y Física del Espacio (IAFE), Buenos Aires, Argentina. Since 1983, she has worked in remote sensing, and since 1997, she has been dedicated to microwave remote sensing. She is currently the PI of national projects and of Space Agencies AO projects. She is also coordinating a technology transfer project related to applications

and quality analysis of the future Argentine SAOCOM SAR mission products.



Marta Borro is pursuing the Ph.D. degree in the eco-hydrogeomorphic approach to shallow lakes classification in the Paraná River Delta region.

She is a Biologist and has been with the University of San Martín, Buenos Aires, Argentina, since 2008.